ChemComm

COMMUNICATION

View Article Online
View Journal | View Issue

Cite this: *Chem. Commun.*, 2020, **56**, 9110

Received 13th May 2020,
Accepted 30th June 2020

DOI: 10.1039/d0cc03427d

rsc.li/chemcomm

Modifying the luminescent properties of a Cu(I) diphosphine complex using ligand-centered reactions in single crystals†

Kyounghoon Lee,[a] Po-Ni Lai,[b] Riffat Parveen,[c] Courtney M. Donahue,[a] Mikayla M. Wymore,[a] Blake A. Massman,[a] Bess Vlaisavljevich,[c] Thomas S. Teets[b] and Scott R. Daly*[a]

Here we report how reactions at a chemically reactive diphosphine shift the long-lived luminescent colour of a crystalline three-coordinate Cu(I) complex from green to blue. The results demonstrate how vapochromism and single-crystal-to-single-crystal transformations can be achieved using ligand-centered reactions.

Luminescent Cu(I) complexes are highly sought after as potential alternatives to those containing iridium, platinum, and ruthenium due to the higher abundance and lower cost of copper. Cu(I) complexes typically exhibit photoluminescence *via* thermally-activated delayed fluorescence (TADF), which occurs when the energy gap between the S_1 and T_1 excited states (ΔE_{ST}) is thermally accessible, and/or by phosphorescence induced by appreciable spin–orbit coupling.[1] This gives rise to widely tuneable emission lifetimes needed for use in diverse applications such as OLEDs,[2] chemical sensing,[3] photosensitizers,[4] and photocatalysis.[5]

A challenge that has limited the use of luminescent Cu(I) complexes is their propensity to adopt tetrahedral coordination geometries that undergo large excited-state geometric distortions that increase non-radiative decay processes and decrease quantum efficiencies.[1a,3a,4c,6] It has been shown, however, that non-radiative decay processes can be suppressed by using ligands with sterically-bulky substituents to form two- or three-coordinate Cu(I) complexes.[6b,7] Another challenge is developing stable and efficient blue emitters, which has proven difficult with noble metal complexes because of energetically low-lying metal-centered (^{3}MC) d–d states that provide an alternate pathway of non-radiative decay.[8] In contrast, d^{10} complexes have no ^{3}MC states, and several efficient Cu(I) blue emitters have been reported.[7e,9]

We recently described a new class of triaminoborane-bridged diphosphine ligands derived from 1,8,10,9-triazaboradecalin (TBD) called TBDPhos.[10] When bound to Ni(II) and Pd(II), phenyl-substituted TBDPhos (^{Ph}TBDPhos) can undergo cooperative ligand-centered reactions with water and alcohols to form *trans* N–H and B–OH or B–OR bonds on the TBD backbone (Scheme 1).[10a] Given that numerous examples of luminescent Cu(I) diphosphine complexes are known,[1a,2d,4c,11] and some form highly emissive three-coordinate complexes,[6b,7d,e] we postulated that ligand-centered reactions in Cu(I) TBDPhos complexes could be used to modify their photophysical properties. Here we report the first such examples using single crystals of (^{Ph}TBDPhos)CuCl (**1**).

Complex **1** was prepared by treating CuCl with ^{Ph}TBDPhos in CH_2Cl_2 (Scheme 1). The reaction was monitored by NMR spectroscopy, and new signals supporting the formation of **1** were observed at δ 24.8 ppm and δ 40.9 ppm in the ^{11}B and ^{31}P NMR spectra, respectively. Light greenish-yellow crystals were grown from CH_2Cl_2 solution by vapor diffusion with Et_2O. As expected, the crystals were highly luminescent, appearing green when exposed to UV light. X-ray diffraction data collected on the crystals revealed the structure to be three-coordinate monomeric **1** (Fig. 1). The geometry around Cu and B are best described

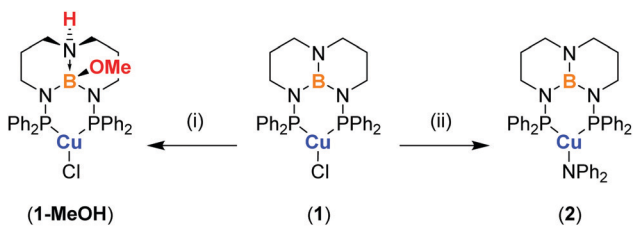

Scheme 1 Structure of (^{Ph}TBDPhos)CuCl (**1**) and synthesis of **1-MeOH** and **2**. (i) Excess MeOH at RT. (ii) Addition of 1 eq. of $HNPh_2$ and $KN(SiMe_3)_2$ in toluene at −78 °C.

[a] *Department of Chemistry, The University of Iowa, E331 Chemistry Building, Iowa City, IA 52242, USA. E-mail: scott-daly@uiowa.edu*
[b] *Department of Chemistry, University of Houston, 3585 Cullen Boulevard, Room 112, Houston, TX 77204, USA*
[c] *Department of Chemistry, The University of South Dakota, 414 E. Clark Street, Vermillion, SD 57069, USA*

† Electronic supplementary information (ESI) available: Experimental details, crystallographic data, NMR spectra, molecular structure of **2**, and *XYZ* coordinates of the calculated structures. CCDC 2003378–2003380. For ESI and crystallographic data in CIF or other electronic format see DOI: 10.1039/d0cc03427d

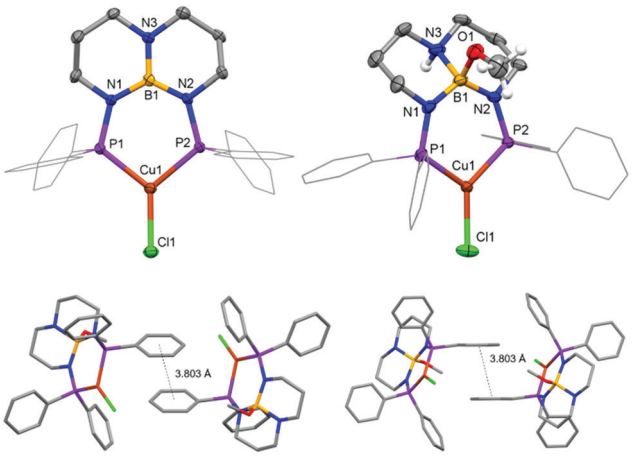

Fig. 1 Top: Molecular structures of **1** (left) and **1-MeOH** (right) with thermal ellipsoids at the 50% probability level. Phenyl groups are depicted as wire frames, and hydrogen atoms except for NH and OCH_3 were omitted from the figures. Bottom: Intermolecular π–π stacking in the extended XRD structure of **1-MeOH**.

as trigonal planar with the sum of the bond angles being 359.81(4)° and 360.0(3)°, respectively, though the three angles around Cu are less congruent due to the ^{Ph}TBDPhos bite angle (P–Cu–P) of 101.52(2)°. The Cu–P bond distances of 2.1952(6) and 2.1953(6) Å are 0.04–0.06 Å shorter compared to other CuCl complexes with aryl-substituted diphosphines.[6b,12]

To give insight into how different ancillary ligands affect the photophysical properties of Cu(I) ^{Ph}TBDPhos complexes, we replaced the chloride in **1** with diphenylamide, another ligand known to yield luminescent Cu(I) complexes with diphosphines.[7e] The synthesis of (^{Ph}TBDPhos)Cu(NPh_2) (**2**) was performed by treating a mixture of **1** and $HNPh_2$ in toluene with $KN(SiMe_3)_2$ at −78 °C, which formed an intense yellow solution (Scheme 1). XRD studies on single crystals obtained by diffusion of pentane into toluene confirmed the three-coordinate complex and revealed similar ^{Ph}TBDPhos bond distances and angles as **1** (Fig. S2; ESI†). Crystals of **2** exhibit similarly green luminescence like **1** despite the change in ancillary ligand.

Although **1** is highly luminescent in the solid-state, its luminescence is dramatically attenuated in solution, which is attributed in part to dynamic changes in its composition and structure when dissolved. NMR analysis of isolated crystals of **1** in CD_2Cl_2 revealed small, broad resonances in the baseline that became more resolved upon cooling (Fig. S6 and S7; ESI†). The ^{31}P NMR spectrum collected at −80 °C for example revealed three resonances, suggesting that monomeric **1** dimerizes to some extent in solution and/or undergoes ligand exchange to form [Cu(^{Ph}TBDPhos)$_2$][$CuCl_2$], as has been reported for other CuCl diphosphine complexes.[13]

Fortunately, the attenuated solution luminescence did not prevent our investigation of ligand-centered reactivity on the photophysical properties of **1**. We discovered that crystals of **1** are not appreciably soluble in MeOH, but soaking them for a few hours to overnight depending on their size changes their photoluminescence from green to blue. To ensure complete conversion, the crystals were soaked for two days and then analyzed by single-crystal XRD. The crystals had the same monoclinic space group as **1** with similar cell parameters, although the cell setting changed from $P2_1/n$ to $P2_1/c$ and the unit cell volume increased from 2850.3(5) to 3017.4(5) Å^3 (Table S1; ESI†). Modeling the crystal data revealed these changes to be due to *trans* addition of MeOH to the TBD backbone to yield (^{Ph}TBDPhos-MeOH)CuCl (**1-MeOH**; Fig. 1). The Cu–P and Cu–Cl distances in **1** and **1-MeOH** are effectively identical (Table S2; ESI†), but the P–Cu–P angle increased from 101.52(2)° in **1** to 105.13(4)° in **1-MeOH**. As expected, the biggest change occurred at the diphosphine. The N–B bond distances of 1.427(3), 1.464(3), and 1.468 Å in **1** increase to 1.628(5), 1.529(5), and 1.544(5) Å in **1-MeOH**.

One of the most remarkable features of the ligand-centered reactivity with **1** is that it also occurs when crystals are exposed to MeOH vapor. Crystal changes that occur in response to vapor are called solvent-induced single-crystal-to-single-crystal (SCSC) transformations.[14] Not surprisingly, the SCSC transformation was slower than that observed when soaking the crystals in MeOH, as followed over the course of several days by the photoluminescent colour change from green to blue. Vapochromism with luminescent Cu(I) complexes is known,[2d,3e,f,15] and it is typically initiated by solvent induced rearrangement of ligands and metal coordination geometry,[16] solvent intercalation in the crystal lattice,[17] or solvent binding at the metal.[18] Complex **1** is unique because it relies on a ligand-centered reaction to induce the SCSC and the vapochromic response with MeOH. The vapochromic reaction with **1** did not appear to be reversible; the blue luminescence persisted when placing **1-MeOH** under dynamic vacuum at *ca.* 10^{-2} Torr overnight. Moreover, the crystals appeared to decompose when heated above 60 °C under vacuum, as indicated by their quenched luminescence.

In contrast to **1**, attempts to test the ligand-centered reactivity of **2** were unsuccessful. Exposing **2** to MeOH, for example, quenched its photoluminescence. Given that Cu–NPh_2 bonds in **2** are highly susceptible to protonolysis, as described previously for similar Cu(I) amido complexes,[7e] and because emission of **2** is quenched in the solid state when exposed to MeOH, we did not pursue further investigations into its reactivity.

Room-temperature excitation of solid samples of **1** at 360 nm yielded an emission peak at 502 nm consistent with its green luminescence (Fig. 2), and triplicate measurements revealed the quantum yield (Φ_{PL}) to be 67(1)%. The emission spectrum for **2** is similar to **1** with λ_{max} = 505 nm and a slight shoulder at 454 nm, but the quantum yield decreased to Φ_{PL} = 33(1)%. The MeOH-bound complex **1-MeOH** showed the most significant change, as expected based on the change in photoluminescence colour; excitation at 310 nm yielded a blue-shifted λ_{max} of 466 nm and Φ_{PL} = 9.2(6)%.

Photoemission decay plots for **1**, **2**, and **1-MeOH** showed bi-exponential curves with weighted-average lifetimes of 670, 550, and 770 μs, respectively. The average radiative decay rates (k_r) decreased across the series in the order **1** > **2** > **1-MeOH** from 1.1×10^3 to 1.3×10^2 s^{-1}, whereas the non-radiative decay rates (k_{nr}) increased from 5.0×10^2 s^{-1} in **1** to 1.2×10^3 s^{-1} in **2** and **1-MeOH** (Table 1). Such long lifetimes suggest that phosphorescence is the dominant photoemission processes,[7g] and the

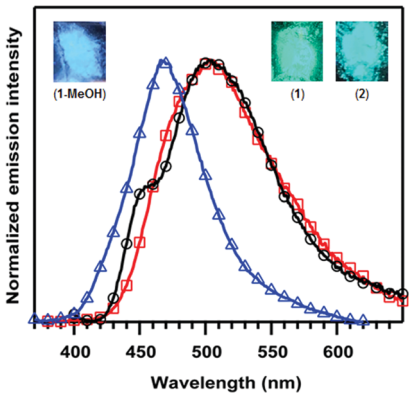

Fig. 2 Emission spectra for **1** (red; □), **2** (black; ○) and **1-MeOH** (blue; △) in the solid-state. Photoluminescence colours for **1**, **2**, and **1-MeOH** are provided at the upper right or left corners of the figure. Data were collected every 1 nm, and the symbols are present to help distinguish the overlaid plots.

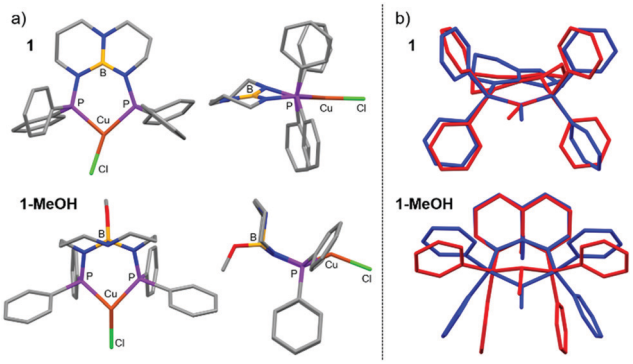

Fig. 3 (a) Top and side views of optimized gas-phase DFT structures for the triplet state (T_1) of **1** (top) and **1-MeOH** (bottom). (b) Stack plot of calculated structures for **1** and **1-MeOH**: gas-phase singlet ground state (S_0; red) and triplet excited state (T_1; blue).

lifetimes are remarkable when combined with their relatively high quantum yields.[7g]

DFT and TDDFT calculations were used to investigate the photophysical differences in **1**, **1-MeOH**, and **2**. The calculations were performed in the gas phase and using SMD solvation models with toluene and CH_2Cl_2 for comparison. Consistent with our solution UV-vis data,[19] analysis of the TDDFT calculations and associated Kohn–Sham orbitals confirm that UV absorptions in **1** are best assigned as MLCT transitions between the HOMO (Cu–Cl π^* and Cu–P σ^*) and unoccupied phenyl-derived π orbitals localized on the ^{Ph}TBDPhos ligand. Despite addition of MeOH to the TBD backbone, the calculated absorption transitions for **1-MeOH** are effectively the same as **1**.

Evaluating the emissive properties of the Cu(I) complexes required determining the structures of their T_1 excited states. The optimized structures revealed that **1** undergoes a distortion from trigonal planar in the ground state to T-shaped in the T_1 state, similar to that reported for other emissive three-coordinate complexes (Fig. 3).[6b,20] The *cis* and *trans* P–Cu–Cl angles were 113.2° and 150.7° and the P–Cu–P angle was 96.1° (Σ = 360.0°). A similar, albeit less dramatic bending distortion was calculated for the T_1 structure of **2**, but also with rotation of the NPh_2 phenyl groups around the Cu–N bond. In contrast to **1** and **2**, **1-MeOH** undergoes a different Jahn–Teller distortion in the excited state. Instead of trigonal planar to T-shaped, the T_1 coordination geometry in **1-MeOH** is trigonal pyramidal with more congruent P–Cu–Cl angles of 123.4° and 119.4° and a P–Cu–P angle of 86.7° (Σ = 329.5°). Given that structural excited-state distortions are known to influence the availability of non-radiative decay modes, it is likely that the different excited-state Jahn–Teller distortions for **1-MeOH** compared to **1** contributes to its decreased quantum yield.

Table 1 Solid-state emission data for **1**, **2**, and **1-MeOH** at room temperature

Complex	λ_{em}/nm	Φ_{PL}	τ/μs	$k_r/10^2$ s^{-1}	$k_{nr}/10^2$ s^{-1}
1	502	0.67(1)	670	11	5
2	454(sh), 505	0.33(1)	550	6.4	12
1-MeOH	466	0.092(6)	770	1.3	12

Calculations performed on discrete complexes of **1** and **1-MeOH** did not offer a clear reason for the colorimetric shift between the two, which suggests that the shift is tied to differences in their extended solid-state structures. The Kohn–Sham orbitals involved in the transitions do not have appreciable boron or nitrogen character in the optimized ground- and excited-state structures, which appears to rule out that the colour change is associated with chemical engagement of boron and nitrogen orbitals on the ligand (Fig. S3 and S4; ESI†). Analysis of the calculated $T_1 \rightarrow S_0$ emission energies was also inconclusive because they varied in magnitude and sign depending on the conditions selected (gas-phase *vs.* solvation model *vs.* solvent selection; Table S4, ESI†). As has been described for luminescent complexes containing aryl-substituted ligands,[17,21] we suspect that the change in luminescence colour can be attributed to solid-state differences in intermolecular π–π stacking between adjacent aryl groups in response to the SCSC transformation. Evidence in support of this hypothesis is afforded by analysis of the XRD data. The crystal structure of **1** shows no intermolecular π–π stacking, whereas the extended structure of **1-MeOH** has adjacent complexes with overlapping, parallel-offset phenyl groups with Ph···Ph centroid distances of 3.803 Å (Fig. 1).

We briefly investigated the scope of the solid-state ligand-centered reactivity of **1** with other Brønsted acids. As with MeOH, the green photoluminescence of crystalline **1** slowly turns blue when exposed to vapor from water and aqueous HCl solutions (Fig. 4). It appears that ^{Ph}TBDPhos in crystals of **1** undergoes solid-state ligand-centered reactions in the same way as it does with MeOH under these conditions, and this observation is consistent with solution reactivity reported previously with (^{Ph}TBDPhos)$NiCl_2$ and (^{Ph}TBDPhos)$PdCl_2$.[10a,b]

In summary, we have described how three-coordinate Cu(I) complexes with a reactive diphosphine ligand called ^{Ph}TBDPhos exhibit green photoemission, relatively high quantum yields, and long luminescent lifetimes. Exposing crystals of **1** to MeOH solution or vapor turns the photoemission blue by way of ligand-centered

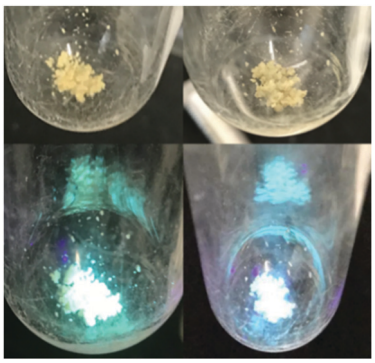

Fig. 4 Single crystals of **1** before (left) and after (right) exposure to vapor from an aqueous HCl solution for 12 h under normal light (top) and commercial violet laser pointer (bottom).

reactions at the TBD backbone that cause a single-crystal-to-single-crystal transformation. Similar ligand-centered reactivity appears to be operative when **1** is exposed to vapor from water and aqueous HCl solutions. Collectively, these results demonstrate how ligand-centered reactions can be used to modify the luminescent properties of crystalline Cu(I) complexes, which may be useful for the development of new materials for optical sensing and luminescent devices.

This work was generously supported by the University of Iowa Center for Health Effects of Environmental Contamination (CHEEC) and the National Science Foundation (1650894). We thank Dale Swenson for collecting the single-crystal XRD data. T. S. T. acknowledges the Welch Foundation (Grant no. E-1887) for funding.

Conflicts of interest

There are no conflicts to declare.

Notes and references

1 (*a*) P. C. Ford, E. Cariati and J. Bourassa, *Chem. Rev.*, 1999, **99**, 3625–3648; (*b*) H. Yersin, *Highly efficient OLEDs with phosphorescent materials/edited by Hartmut Yersin*, Wiley-VCH Verlag GmbH & Co. KgaA, Weinheim, Germany, 2008; (*c*) M. Wallesch, D. Volz, D. M. Zink, U. Schepers, M. Nieger, T. Baumann and S. Bräse, *Chem. – Eur. J.*, 2014, **20**, 6578–6590; (*d*) W. Liu, Y. Fang and J. Li, *Adv. Funct. Mater.*, 2018, **28**, 1705593; (*e*) L. P. Ravaro, K. P. S. Zanoni and A. S. S. de Camargo, *Energy Rep.*, 2020, **6**, 37–45.

2 (*a*) M. J. Leitl, D. M. Zink, A. Schinabeck, T. Baumann, D. Volz and H. Yersin, *Top. Curr. Chem.*, 2016, **374**, 25; (*b*) H. Yersin, A. F. Rausch, R. Czerwieniec, T. Hofbeck and T. Fischer, *Coord. Chem. Rev.*, 2011, **255**, 2622–2652; (*c*) F. Dumur, *Org. Electron.*, 2015, **21**, 27–39; (*d*) E. Cariati, E. Lucenti, C. Botta, U. Giovanella, D. Marinotto and S. Righetto, *Coord. Chem. Rev.*, 2016, **306**, 566–614.

3 (*a*) D. R. McMillin and K. M. McNett, *Chem. Rev.*, 1998, **98**, 1201–1220; (*b*) M. H. Keefe, K. D. Benkstein and J. T. Hupp, *Coord. Chem. Rev.*, 2000, **205**, 201–228; (*c*) E. J. O'Neil and B. D. Smith, *Coord. Chem. Rev.*, 2006, **250**, 3068–3080; (*d*) Q. Zhao, F. Li and C. Huang, *Chem. Soc. Rev.*, 2010, **39**, 3007–3030; (*e*) O. S. Wenger, *Chem. Rev.*, 2013, **113**, 3686–3733; (*f*) A. Kobayashi and M. Kato, *Chem. Lett.*, 2017, **46**, 154–162.

4 (*a*) N. Armaroli, *Chem. Soc. Rev.*, 2001, **30**, 113–124; (*b*) S.-P. Luo, E. Mejía, A. Friedrich, A. Pazidis, H. Junge, A.-E. Surkus, R. Jackstell, S. Denurra, S. Gladiali, S. Lochbrunner and M. Beller, *Angew. Chem., Int. Ed.*, 2012, **52**, 419–423; (*c*) Y. Zhang, M. Schulz, M. Wächtler, M. Karnahl and B. Dietzek, *Coord. Chem. Rev.*, 2018, **356**, 127–146.

5 (*a*) *Chemical Photocatalysis*, ed. B. König, de Gruyter, 2013; (*b*) S. Paria and O. Reiser, *ChemCatChem*, 2014, **6**, 2477–2483; (*c*) S. E. Creutz, K. J. Lotito, G. C. Fu and J. C. Peters, *Science*, 2012, **338**, 647; (*d*) Q. M. Kainz, C. D. Matier, A. Bartoszewicz, S. L. Zultanski, J. C. Peters and G. C. Fu, *Science*, 2016, **351**, 681.

6 (*a*) N. Armaroli, G. Accorsi, F. Cardinali and A. Listorti, *Top. Curr. Chem.*, 2007, **280**, 69–115; (*b*) M. Hashimoto, S. Igawa, M. Yashima, I. Kawata, M. Hoshino and M. Osawa, *J. Am. Chem. Soc.*, 2011, **133**, 10348–10351; (*c*) M. Iwamura, S. Takeuchi and T. Tahara, *J. Am. Chem. Soc.*, 2007, **129**, 5248–5256.

7 (*a*) V. A. Krylova, P. I. Djurovich, M. T. Whited and M. E. Thompson, *Chem. Commun.*, 2010, **46**, 6696–6698; (*b*) R. Hamze, R. Jazzar, M. Soleilhavoup, P. I. Djurovich, G. Bertrand and M. E. Thompson, *Chem. Commun.*, 2017, **53**, 9008–9011; (*c*) S. Shi, P. I. Djurovich and M. E. Thompson, *Inorg. Chim. Acta*, 2018, **482**, 246–251; (*d*) M. Osawa, *Chem. Commun.*, 2014, **50**, 1801–1803; (*e*) K. J. Lotito and J. C. Peters, *Chem. Commun.*, 2010, **46**, 3690–3692; (*f*) S. Shi, L. R. Collins, M. F. Mahon, P. I. Djurovich, M. E. Thompson and M. K. Whittlesey, *Dalton Trans.*, 2017, **46**, 745–752; (*g*) R. Hamze, J. L. Peltier, D. Sylvinson, M. Jung, J. Cardenas, R. Haiges, M. Soleilhavoup, R. Jazzar, P. I. Djurovich, G. Bertrand and M. E. Thompson, *Science*, 2019, **363**, 601–606; (*h*) S. Shi, M. C. Jung, C. Coburn, A. Tadle, M. R. Daniel Sylvinson, P. I. Djurovich, S. R. Forrest and M. E. Thompson, *J. Am. Chem. Soc.*, 2019, **141**, 3576–3588.

8 (*a*) H. Na and T. S. Teets, *J. Am. Chem. Soc.*, 2018, **140**, 6353–6360; (*b*) T. Sajoto, P. I. Djurovich, A. B. Tamayo, J. Oxgaard, W. A. Goddard and M. E. Thompson, *J. Am. Chem. Soc.*, 2009, **131**, 9813–9822; (*c*) K. P. S. Zanoni, R. L. Coppo, R. C. Amaral and N. Y. Murakami Iha, *Dalton Trans.*, 2015, **44**, 14559–14573.

9 (*a*) M. J. Leitl, F.-R. Küchle, H. A. Mayer, L. Wesemann and H. Yersin, *J. Phys. Chem. A*, 2013, **117**, 11823–11836; (*b*) T. Hofbeck, U. Monkowius and H. Yersin, *J. Am. Chem. Soc.*, 2015, **137**, 399–404; (*c*) T. Gneuß, M. J. Leitl, L. H. Finger, H. Yersin and J. Sundermeyer, *Dalton Trans.*, 2015, **44**, 20045–20055; (*d*) A. Schinabeck, N. Rau, M. Klein, J. Sundermeyer and H. Yersin, *Dalton Trans.*, 2018, **47**, 17067–17076.

10 (*a*) K. Lee, C. M. Donahue and S. R. Daly, *Dalton Trans.*, 2017, **46**, 9394–9406; (*b*) K. Lee, C. Kirkvold, B. Vlaisavljevich and S. R. Daly, *Inorg. Chem.*, 2018, **57**, 13188–13200; (*c*) K. Lee, C. W. Kim, J. L. Buckley, B. Vlaisavljevich and S. R. Daly, *Dalton Trans.*, 2019, **48**, 3777–3785.

11 (*a*) V. W.-W. Yam, V. K.-M. Au and S. Y.-L. Leung, *Chem. Rev.*, 2015, **115**, 7589–7728; (*b*) R. Czerwieniec, M. J. Leitl, H. H. H. Homeier and H. Yersin, *Coord. Chem. Rev.*, 2016, **325**, 2–28; (*c*) K. Tsuge, Y. Chishina, H. Hashiguchi, Y. Sasaki, M. Kato, S. Ishizaka and N. Kitamura, *Coord. Chem. Rev.*, 2016, **306**, 636–651; (*d*) C. Kutal, *Coord. Chem. Rev.*, 1990, **99**, 213–252.

12 S. Daly, M. F. Haddow, A. G. Orpen, G. T. A. Rolls, D. F. Wass and R. L. Wingad, *Organometallics*, 2008, **27**, 3196–3202.

13 (*a*) K. Saito, S. Saijo, K. Kotera and T. Date, *Chem. Pharm. Bull.*, 1985, **33**, 1342–1350; (*b*) P. C. Healy, J. C. McMurtrie and J. Bouzaid, *Acta Crystallogr., Sect. E: Crystallogr. Commun.*, 2010, **66**, m493–m494.

14 A. Chaudhary, A. Mohammad and S. M. Mobin, *Cryst. Growth Des.*, 2017, **17**, 2893–2910.

15 (*a*) X. Zhang, B. Li, Z.-H. Chen and Z.-N. Chen, *J. Mater. Chem.*, 2012, **22**, 11427–11441; (*b*) E. Li, K. Jie, M. Liu, X. Sheng, W. Zhu and F. Huang, *Chem. Soc. Rev.*, 2020, **49**, 1517–1544.

16 (*a*) E. Cariati, X. Bu and P. C. Ford, *Chem. Mater.*, 2000, **12**, 3385–3391; (*b*) E. Cariati and J. Bourassa, *Chem. Commun.*, 1998, 1623–1624.

17 X.-W. Chen, H.-L. Yuan, L.-H. He, J.-L. Chen, S.-J. Liu, H.-R. Wen, G. Zhou, J.-Y. Wang and W.-Y. Wong, *Inorg. Chem.*, 2019, **58**, 14478–14489.

18 T. Hasegawa, A. Kobayashi, H. Ohara, M. Yoshida and M. Kato, *Inorg. Chem.*, 2017, **56**, 4928–4936.

19 See ESI† for details.

20 K. A. Barakat, T. R. Cundari and M. A. Omary, *J. Am. Chem. Soc.*, 2003, **125**, 14228–14229.

21 (*a*) K.-H. Wong, K.-K. Cheung, M. C.-W. Chan and C.-M. Che, *Organometallics*, 1998, **17**, 3505–3511; (*b*) W. Lu, M. C. W. Chan, K.-K. Cheung and C.-M. Che, *Organometallics*, 2001, **20**, 2477–2486; (*c*) E. A. Mikhalyova, A. V. Yakovenko, M. Zeller, M. A. Kiskin, Y. V. Kolomzarov, I. L. Eremenko, A. W. Addison and V. V. Pavlishchuk, *Inorg. Chem.*, 2015, **54**, 3125–3133.